



HAL
open science

Direct evidence of imprinted vortex states in the antiferromagnet of exchange biased microdisks

G. Salazar-Alvarez, J. Kavich, J. Sort, A. Mugarza, S. Stepanow, A. Potenza, H. Marchetto, S. S. Dhesi, Vincent Baltz, B. Dieny, et al.

► **To cite this version:**

G. Salazar-Alvarez, J. Kavich, J. Sort, A. Mugarza, S. Stepanow, et al.. Direct evidence of imprinted vortex states in the antiferromagnet of exchange biased microdisks. *Applied Physics Letters*, 2009, 95, pp.012510. 10.1063/1.3168515 . hal-01683831

HAL Id: hal-01683831

<https://hal.science/hal-01683831>

Submitted on 25 May 2019

HAL is a multi-disciplinary open access archive for the deposit and dissemination of scientific research documents, whether they are published or not. The documents may come from teaching and research institutions in France or abroad, or from public or private research centers.

L'archive ouverte pluridisciplinaire **HAL**, est destinée au dépôt et à la diffusion de documents scientifiques de niveau recherche, publiés ou non, émanant des établissements d'enseignement et de recherche français ou étrangers, des laboratoires publics ou privés.

Direct evidence of imprinted vortex states in the antiferromagnet of exchange biased microdisks

G. Salazar-Alvarez,^{1,2} J. J. Kavich,^{1,a)} J. Sort,^{3,4,b)} A. Mugarza,¹ S. Stepanow,¹ A. Potenza,⁵ H. Marchetto,⁵ S. S. Dhesi,⁵ V. Baltz,⁶ B. Dieny,⁶ A. Weber,⁷ L. J. Heyderman,⁷ J. Nogués,^{1,3} and P. Gambardella^{1,3}

¹Centre d'Investigació en Nanociència i Nanotecnologia (ICN-CSIC), Campus UAB, E-08193 Barcelona, Spain

²Department of Materials Science and Engineering, Royal Institute of Technology, S-10044 Stockholm, Sweden

³Institució Catalana de Recerca i Estudis Avançats (ICREA), E-08010 Barcelona, Spain

⁴Departament de Física, Universitat Autònoma de Barcelona, E-08193, Barcelona, Spain

⁵Diamond Light Source, Chilton, Didcot, Oxfordshire, OX11 0DE, United Kingdom

⁶SPINTEC (URA 2512 CNRS/CEA), CEA/Grenoble, 17 Rue des Martyrs, 38054 Grenoble Cedex 9, France

⁷Laboratory for Micro- and Nanotechnology, Paul Scherrer Institut, CH-5232 Villigen PSI, Switzerland

(Received 10 April 2009; accepted 15 June 2009; published online 10 July 2009)

The magnetic domain structure of patterned antiferromagnetic/ferromagnetic Ir₂₀Mn₈₀/Ni₈₀Fe₂₀ bilayer microdisk arrays has been investigated using layer-specific polarized x-ray photoemission electron microscopy and magnetic circular dichroism. Magnetic imaging at the Fe and Mn *L*-edge resonances provided direct evidence of a vortex state imprinted into the antiferromagnet at the interface. The opposite magnetic contrast between the layers indicated a reversed chirality of the imprinted vortex state, and a quantitative analysis of the magnetic moment from the dichroism spectra showed that uncompensated Mn spins equivalent to about 60% of a monolayer of bulk Ir₂₀Mn₈₀ contributed to the imprinted information at the interface. © 2009 American Institute of Physics. [DOI: 10.1063/1.3168515]

The phenomenon of exchange bias has been extensively studied over the past decades.^{1,2} Recently, though, investigation of the exchange coupling of *laterally confined* bilayer antiferromagnetic (AFM)/ferromagnetic (FM) structures has been driven by the technological importance of continually overcoming scaling barriers in magnetic information storage as well as the interest in fundamental properties directly related to the low dimensionality.^{3–6} It is generally accepted that uncompensated spins located at the AFM/FM interface are responsible for the exchange coupling.^{7,8} However, their role in the formation of magnetic domain structures and related reversal processes is not well understood, motivating ongoing investigations in these topics.

We have previously studied the evolution of magnetization states in micron-sized disks composed of FM NiFe (Ni₈₀Fe₂₀) and AFM IrMn (Ir₂₀Mn₈₀).^{9–14} Upon field-cooling the microdisks in nonsaturating fields, it was possible to obtain a new asymmetric switching mode characterized by a modified constricted magnetization loop particular to the vortex state.¹⁰ Furthermore, under zero-field-cooled (ZFC) conditions, the stability of the vortex state was enhanced, i.e., both the nucleation and annihilation fields were increased with respect to pristine unbiased NiFe disks.^{10,11} These results suggest that during the cooling procedures, nonuniform magnetization states (e.g., vortices or displaced vortices) are *imprinted* into the AFM. Although micromagnetic simulations corroborate this picture, evidence of imprinted vortex states in the AFM has not been realized. Additionally, without an explicit driver for domain formation, domains in AFMs typically originate from random nucle-

ation due to defects¹⁵ and are not expected to form closed-flux states.

In this letter, it is shown that spontaneous vortex states formed in a ZFC FM NiFe layer are imprinted into uncompensated spins at the interface with an AFM IrMn layer. Magnetic contrast imaging using element-specific polarized x-ray photoemission electron microscopy (XPEEM) shows vortex states of opposite chirality in the FM and AFM layers. From a quantitative analysis of the *L*-edge x-ray magnetic circular dichroism (XMCD), the fraction of Mn atoms that participate in the formation of the imprinted vortex is equivalent to about 60% of a monolayer of bulk IrMn. The occurrence of exchange biased vortices in IrMn/NiFe microdisks is also found to depend strongly on their lateral dimension.

Thin films of Ta(5 nm)/Cu(3 nm)/IrMn(5 nm)/NiFe(6 nm)/Al(1.5 nm) were deposited on a naturally oxidized Si(100) wafer by sputtering stoichiometric targets. Arrays of 500 nm, 1, 2, 3, and 4 μm diameter circular disks, separated by a distance equal to the diameter, were patterned by e-beam lithography combined with a lift-off process. The samples were prepared analogously to those previously studied¹⁰ with the exceptions that the order of the FM and AFM layers was reversed and the thickness of the NiFe was reduced from 12 to 6 nm to optimize the sensitivity of the XPEEM to Mn spins at the IrMn/NiFe interface. The patterned arrays were demagnetized at 550 K, above the blocking temperature of the bilayer, and subsequently ZFC to room temperature. Magnetic characterization prior to x-ray measurements using magneto-optical Kerr effect revealed constricted hysteresis loops expected from the previous experiments and simulations of exchange coupled vortices.¹⁰

XPEEM imaging experiments were carried out at beamline I06 at the Diamond Light Source. Element-specific im-

^{a)}Electronic mail: jerald.kavich.icn@uab.es.

^{b)}Electronic mail: jordi.sort@uab.es.

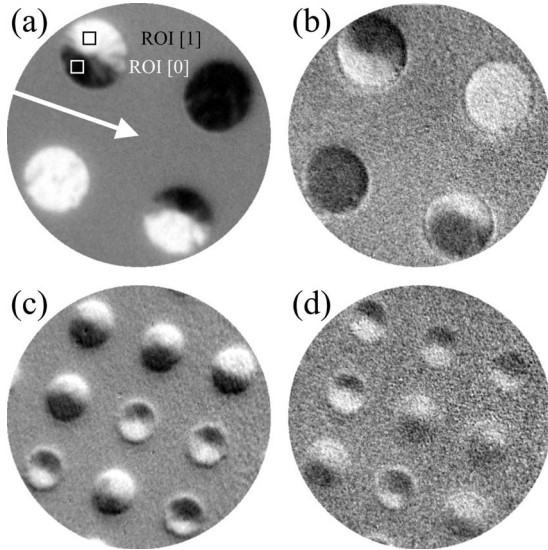


FIG. 1. Magnetic contrast images were acquired at the Fe (a) and Mn (b) resonance energies on the 2 μm bilayer disks. The images at the Fe and Mn edges for the 1 μm diameter disks are shown in (c) and (d), respectively. The arrow indicates the direction of propagation of the x-ray beam.

ages were acquired at the Fe, Ni, and Mn L -edge resonances for right- and left-circularly polarized x-rays, P^+ and P^- , respectively. At the Mn edge, for example, the normalized intensity image for right-circular polarization is defined as $P^+ = P^+_{638 \text{ eV}} / P^+_{630 \text{ eV}}$, where $P^+_{638 \text{ eV}}$ and $P^+_{630 \text{ eV}}$ correspond to the maximum XMCD and the pre-edge intensity, respectively. The magnetic contrast images, shown in Fig. 1, were subsequently constructed using $(P^+ - P^-) / (P^+ + P^-)$. It should be noted that by measuring secondary photoemitted electrons, XPEEM is an inherently surface-sensitive technique whose probing depth decays as $\exp[-z/\lambda]$, where λ is the mean free path of the electrons. Hence, even samples with optimized layer ordering and thicknesses required long integration times to achieve sufficient dichroic contrast. Here, each Mn image was constructed from 1000 images using an acquisition time of 2 s per image.

Due to the element-specificity of the x-ray absorption edges, the Fe and Ni edges probe only the FM NiFe layer, while the Mn edge gives information unique to the AFM IrMn layer. Vortex structures were clearly observed in the NiFe layer in the 500 nm (not shown), 1 μm , and 2 μm microdisk arrays as shown in Figs. 1(a) and 1(c). The resulting XPEEM images at the Mn edge [Figs. 1(b) and 1(d)] show unambiguous evidence of magnetic vortex states of opposite contrast and hence antiparallel coupling to those observed at the Fe (and Ni, not shown) edge for the FM layer. This AFM coupling is unusual¹⁶ and has been shown to depend on material parameters in IrMn-based systems.¹⁷ In our case, we note that AFM coupling is also observed in structures with uniform magnetization and multiple domain states.

To investigate the origin of the imprinted AFM domain structure, we used x-ray absorption spectroscopy (XAS) across both the Fe and Mn resonance energies. The absorption spectra were derived from a series of XPEEM images, taken as a function of energy, by integrating the intensity over high-contrast regions-of-interest (ROIs) in each image. This allows XAS and XMCD spectra to be obtained with high spatial resolution. The XAS and XMCD presented in

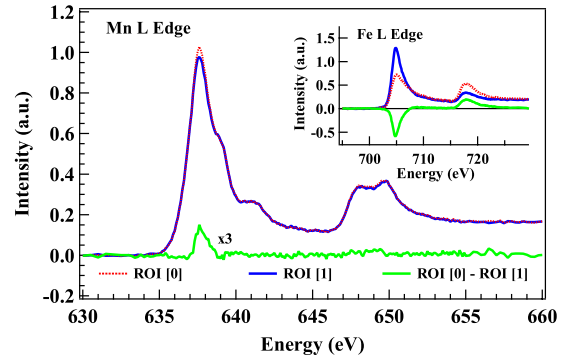


FIG. 2. (Color online) Spatially resolved XAS and XMCD acquired at the Mn $L_{3,2}$ edges using right-circularly polarized light taken within a single disk containing a vortex configuration specified in Fig. 1(a). The Mn XAS and XMCD display a lineshape similar to the spectra previously reported in similarly patterned¹⁸ and unpatterned bilayer IrMn films.¹⁷

Fig. 2 were obtained using the two ROIs defined within a single microdisk displaying a vortex configuration specified in Fig. 1(a). The Mn XAS and XMCD display a lineshape similar to the spectra previously reported in similarly patterned¹⁸ and unpatterned bilayer IrMn films.¹⁷

As expected from the reversed contrast of the Fe and Mn XPEEM images in Fig. 1, we find that the sign of the Mn XMCD spectra is opposite with respect to Fe (inset of Fig. 2). Since bulk $\text{Ir}_{20}\text{Mn}_{80}$ possesses a noncollinear spin-density wave structure leading to zero XMCD (and linear dichroism) contrast,¹⁹ the nonzero Mn XMCD is attributed to the presence of uncompensated spins at the IrMn/NiFe interface. In the absence of applied field, both pinned and unpinned interfacial spins contribute to the XMCD. To estimate the total quantity of uncompensated spins in the AFM layer involved in the imprinted structures, a Mn moment of 0.11 μ_B/Mn ion was calculated using XMCD sum rule analysis. The Mn spin moment, however, is known to be *underestimated* by the sum rules, and an experimental correction factor of ~ 1.8 has been determined.²⁰ Additionally, the electron signal is an exponentially weighted average from the entire IrMn layer with a characteristic length defined by the electron mean free path, which is further attenuated by the NiFe (6 nm) and Al (1.5 nm) overlayers. To estimate the amount of uncompensated spins at the interface, we correct for these effects with a simple model²¹ and assume that the uncompensated spins are located in the first IrMn layer with magnetic moments equal to Mn in bulk IrMn.²² The fraction of uncompensated spins is found to be $60 \pm 20\%$ of a monolayer, which is clear evidence that the vortex state is imprinted into uncompensated moments near the interface. This value is consistent with those previously reported for exchange biased films and patterned structures displaying single domain states.^{8,17,18}

Due to the weighted depth-sensitivity of XPEEM and complex AFM structure of IrMn, we cannot conclude on the persistence of the vortexlike AFM alignment of the Mn spins into the IrMn layer. However, measurements carried out on the reversed layer structure, Ta(5 nm)/Cu(3 nm)/NiFe(12 nm)/IrMn(5 nm)/Al(1.5 nm), exclude the possibility that the *uncompensated* vortex state extends throughout the IrMn layer.

As for purely FM structures,^{23–25} the set of patterned array structures demonstrates that vortex stability in FM/AFM confined systems strongly depends on the geometry. The microdisk arrays here, all with 6 nm NiFe thick layers,

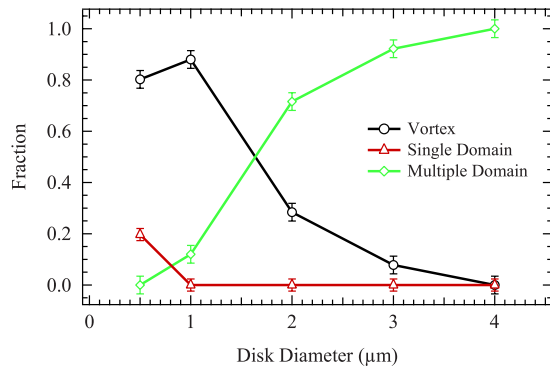


FIG. 3. (Color online) Fraction of disks with either single-, vortex-, or multidomain states. The error was calculated as the maximum value of $\sqrt{[f(1-f)/N]}$, where f is the frequency with which a particular state is counted and N is the total number of disks for each diameter.

exhibit an optimum diameter for vortex formation around 1 μm (see Fig. 3). Below this critical dimension, single domain structures start to become apparent. Above 1 μm , the high resolution XPEEM images show regions of different contrasts, with length scales on the order of 50–100 nm within the disks, indicating the onset of multiple domain states as seen in the lower left disk in Fig. 1(a). At present, no systematic investigation of the occurrence of vortex states in FM/AFM disks versus FM disks exists; however, the optimal size for the formation of exchange coupled closed-flux states depends on the competition between exchange and shape anisotropy^{5,6} so that deviations from the FM case are expected depending on the AFM material.

To conclude, magnetic contrast XPEEM images at the Fe (NiFe) and Mn (IrMn) resonant energies illustrate the first direct evidence of the presence of imprinted vortices in patterned AFM/FM bilayer structures previously investigated by Kerr and magnetic force microscopy. The chirality of the vortex imprinted into the AFM is found to be opposite to that of the NiFe layer. The origin of the imprinted closed-flux states in IrMn is ascribed to the presence of uncompensated Mn spins at the IrMn/NiFe interface, which couple antiferromagnetically to the NiFe layer. The formation of the AFM/FM vortex structures is found to depend critically on the disk size with an optimum diameter of 1 μm for NiFe (6 nm)/IrMn (5 nm) bilayers.

This work was carried out with the support of Diamond Light Source, the Spanish MICINN (Grant No. MAT2007-

66302-C02), and the European Research Council (Starting Grant 203239).

- ¹J. Nogués and I. K. Schuller, *J. Magn. Magn. Mater.* **192**, 203 (1999).
- ²A. E. Berkowitz and K. Takano, *J. Magn. Magn. Mater.* **200**, 552 (1999).
- ³J. Nogués, J. Sort, V. Langlais, V. Skumryev, S. Suriñach, J. S. Muñoz, and M. D. Baró, *Phys. Rep.* **422**, 65 (2005).
- ⁴J. Eisenmenger, Z.-P. Li, W. A. A. Macedo, and I. K. Schuller, *Phys. Rev. Lett.* **94**, 057203 (2005).
- ⁵W. Jung, F. J. Castaño, and C. A. Ross, *Phys. Rev. Lett.* **97**, 247209 (2006).
- ⁶C. M. Schneider, O. de Haas, D. Tietjen, U. Muschiol, N. Cramer, Z. Celinski, A. Oelsner, M. Klais, C. Zieten, O. Schmidt, G. Schönhense, N. Zema, and S. Zennaro, *J. Phys. D* **35**, 2472 (2002).
- ⁷K. Takano, R. H. Kodama, A. E. Berkowitz, W. Cao, and G. Thomas, *Phys. Rev. Lett.* **79**, 1130 (1997).
- ⁸H. Ohldag, A. Scholl, F. Nolting, E. Arenholz, S. Maat, A. T. Young, M. Carey, and J. Stohr, *Phys. Rev. Lett.* **91**, 017203 (2003).
- ⁹J. Sort, A. Hoffmann, S. H. Chung, K. S. Buchanan, M. Grimsditch, M. D. Baró, B. Dieny, and J. Nogués, *Phys. Rev. Lett.* **95**, 067201 (2005).
- ¹⁰J. Sort, K. S. Buchanan, V. Novosad, A. Hoffmann, G. Salazar-Alvarez, A. Boller, M. D. Baró, B. Dieny, and J. Nogués, *Phys. Rev. Lett.* **97**, 067201 (2006).
- ¹¹J. Sort, G. Salazar-Alvarez, M. D. Baró, B. Dieny, A. Hoffmann, V. Novosad, and J. Nogués, *Appl. Phys. Lett.* **88**, 042502 (2006).
- ¹²A. Hoffmann, J. Sort, K. S. Buchanan, and J. Nogués, *IEEE Trans. Magn.* **44**, 1968 (2008).
- ¹³J. Sort, K. S. Buchanan, J. E. Pearson, A. Hoffmann, E. Menéndes, G. Salazar-Alvarez, M. D. Baró, M. Miron, B. Rodmacq, B. Dieny, and J. Nogués, *J. Appl. Phys.* **103**, 07C109 (2008).
- ¹⁴M. Tanase, A. K. Petford-Long, O. Heinonen, K. S. Buchanan, J. Sort, and J. Nogués, *Phys. Rev. B* **79**, 014436 (2009).
- ¹⁵W. Kleemann, *Int. J. Mod. Phys. B* **7**, 2469 (1993).
- ¹⁶E. Arenholz, K. Liu, Z. P. Li, and I. K. Schuller, *Appl. Phys. Lett.* **88**, 072503 (2006).
- ¹⁷M. Tsunoda, S. Yoshitaki, Y. Ashizawa, C. Mitsumata, T. Nakamura, H. Osawa, T. Hirono, D. Y. Kim, and M. Takahashi, *J. Appl. Phys.* **101**, 09E510 (2007).
- ¹⁸T. Eimüller, T. Kato, T. Mizuno, S. Tsunashima, C. Quitmann, T. Rasmvik, S. Iwata, and G. Schutz, *Appl. Phys. Lett.* **85**, 2310 (2004).
- ¹⁹A. Sakuma, K. Fukamichi, K. Sasao, and R. Y. Umetsu, *Phys. Rev. B* **67**, 024420 (2003).
- ²⁰P. Gambardella, H. Brune, S. S. Dhesi, P. Bencok, S. R. Krishnakumar, S. Gardonio, M. Veronese, C. Grazioli, and C. Carbone, *Phys. Rev. B* **72**, 045337 (2005).
- ²¹R. Nakajima, J. Stöhr, and Y. U. Idzerda, *Phys. Rev. B* **59**, 6421 (1999).
- ²²T. Yamaoka, M. Mekata, and H. Takaki, *J. Phys. Soc. Jpn.* **36**, 438 (1974).
- ²³R. P. Cowburn, D. K. Koltsov, A. O. Adeyeye, and M. E. Welland, *Phys. Rev. Lett.* **83**, 1042 (1999).
- ²⁴M. Schneider, H. Hoffmann, S. Otto, T. Haug, and J. Zweck, *J. Appl. Phys.* **92**, 1466 (2002).
- ²⁵P. Vavassori, N. Zaluzec, V. Metlushko, V. Novosad, B. Ilic, and M. Grimsditch, *Phys. Rev. B* **69**, 214404 (2004).